

# Probing of single quantum dot dressed states via an off-resonant cavity

Arka Majumdar,<sup>1,\*</sup> Alexander Papageorge,<sup>1</sup> Erik D. Kim,<sup>1</sup> Michal Bajcsy,<sup>1</sup> Hyochul Kim,<sup>2</sup>  
 Pierre Petroff,<sup>2</sup> and Jelena Vučković<sup>1</sup>

<sup>1</sup>*E. L. Ginzton Laboratory, Stanford University, Stanford, California 94305, USA*

<sup>2</sup>*Materials Department, University of California, Santa Barbara, California 93106, USA*

(Received 17 May 2011; published 22 August 2011)

In recent experiments on coupled quantum dot (QD) optical cavity systems, a pronounced interaction between the dot and the cavity has been observed even for detunings of many cavity linewidths. This interaction has been attributed to an incoherent phonon-mediated scattering process and is absent in atomic systems. Here, we demonstrate that despite its incoherent nature, this process preserves the signatures of coherent interaction between a QD and a strong driving laser, which may be observed via the optical emission from the off-resonant cavity. Under bichromatic driving of the QD, the cavity emission exhibits spectral features consistent with optical dressing of the QD transition. These cavity emission measurements are more akin to absorption measurements of a strongly driven QD rather than resonance fluorescence measurements. In addition to revealing new aspects of the off-resonant QD-cavity interaction, this result provides a new, simpler means of coherently probing QDs and opens the possibility of employing off-resonant cavities to optically interface QD nodes in quantum networks.

DOI: [10.1103/PhysRevB.84.085310](https://doi.org/10.1103/PhysRevB.84.085310)

PACS number(s): 73.21.La, 68.65.Hb, 71.36.+c

## I. INTRODUCTION

Optically controlled quantum dot (QD) spins coupled to semiconductor microcavities constitute a promising platform for robust and scalable quantum information processing devices, where QD spin nodes are optically interconnected via photonic circuits. As such, in recent years much effort has been dedicated to demonstrating fast optical control of a QD spin<sup>1,2</sup> and to studying QD-cavity quantum electrodynamics (CQED) phenomena.<sup>3</sup> The prospect of strongly enhanced light-matter interactions between a QD and an optical field has served as a focal impetus in integrating QDs with high quality factor ( $Q$ ) optical cavities, with maximum enhancement occurring when the QD and the cavity are resonant and the QD is spatially aligned to the cavity mode. Since achieving this maximum enhancement is difficult due to limitations in growth and fabrication techniques, the recently observed coupling between a single QD and a detuned optical cavity mode<sup>4,5</sup> has spurred considerable theoretical<sup>6,7</sup> and experimental interest in determining the physical mechanism behind such coupling as well as in possible applications. Though recent experiments have investigated the linewidth and saturation behavior of this off-resonant cavity emission,<sup>8,9</sup> relatively little has been done to investigate the potential utility of such measurements in performing coherent optical spectroscopy of single QDs.

Here, we present both theoretical and experimental studies of a strongly driven QD that is off-resonantly coupled to a photonic crystal (PC) cavity mode. In these studies, a strong narrow-bandwidth CW (continuous wave) pump laser serves to dress the QD, while a weaker CW probe laser is scanned across the QD resonance; the output signal is always collected at the frequency of the spectrally detuned cavity [Fig. 1(a)]. We theoretically model the bichromatic driving of the QD coupled to an off-resonant cavity by adding an incoherent phonon-mediated coupling between the QD and the cavity and perform simulations with realistic system parameters. The bichromatic driving of a two-level system has been analyzed before.<sup>10</sup> We use similar techniques to analyze the driving of

a two-level system such as a QD, incoherently coupled to an off-resonant cavity via phonons.<sup>7</sup>

## II. THEORY

The dynamics of a driven QD-cavity system is given by the Jaynes-Cummings Hamiltonian:

$$H = \omega_{\text{cav}} a^\dagger a + \omega_{QD} \sigma^\dagger \sigma + g(\sigma^\dagger a + \sigma a^\dagger) + J\sigma + J^* \sigma^\dagger, \quad (1)$$

where  $\omega_{\text{cav}}$  and  $\omega_{QD}$  are, respectively, the cavity and the dot resonance frequency;  $a$  and  $\sigma$  are, respectively, the annihilation operator for a cavity photon and the lowering operator for the QD;  $g$  is the coherent interaction strength between the QD and the cavity; and  $J$  is the Rabi frequency of the driving laser. For bichromatic driving, the driving field  $J$  consists of a strong pump laser with Rabi frequency  $J_1$  tuned to the QD resonance and a weak probe laser with Rabi frequency  $J_2$ , which can be tuned to arbitrary frequency, parameterized by the pump-probe detuning  $\delta$ :

$$J = J_1 e^{i\omega_{QD}t} + J_2 e^{i(\omega_{QD} + \delta)t}. \quad (2)$$

In a frame rotating with the pump laser frequency the Hamiltonian is

$$H = H_0 + H(t) = \Delta a^\dagger a + g(\sigma^\dagger a + \sigma a^\dagger) + J_1 \sigma_x + J_2 (e^{i\delta t} \sigma + e^{-i\delta t} \sigma^\dagger),$$

where  $\Delta = \omega_{\text{cav}} - \omega_{QD}$  is the QD-cavity detuning. We note that for bichromatic driving, the Hamiltonian is always time dependent. To treat incoherent processes we use the master equation<sup>11</sup>

$$\dot{\rho} = -i[H, \rho] + \mathcal{D}(\sqrt{2\gamma}\sigma) + \mathcal{D}(\sqrt{2k}a) + \mathcal{D}(\sqrt{2\gamma_r \bar{n}} a^\dagger \sigma) + \mathcal{D}(\sqrt{2\gamma_r (1 + \bar{n})} a \sigma^\dagger) + \mathcal{D}(\sqrt{2\gamma_d} \sigma^\dagger \sigma),$$

where  $\mathcal{D}(C)$  is the Lindblad term  $C\rho C^\dagger - \frac{1}{2}(C^\dagger C\rho + \rho C^\dagger C)$  associated with the collapse operator  $C$ . The first two terms represent QD spontaneous emission with a rate  $2\gamma$  and cavity

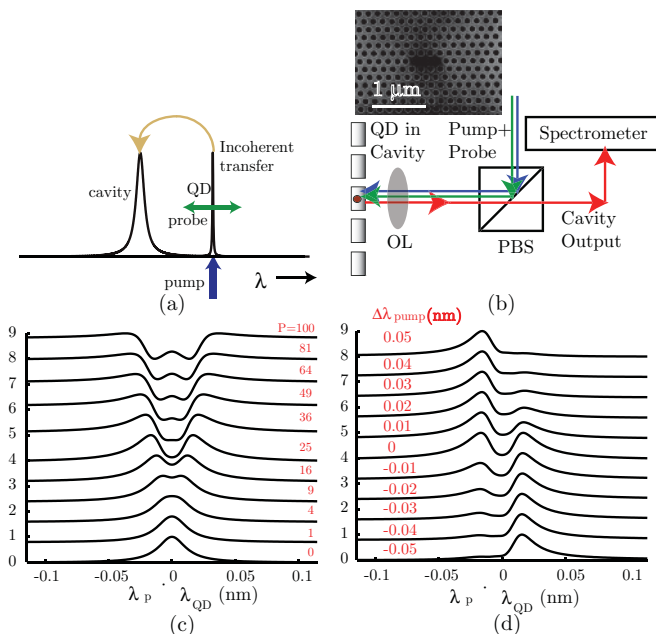


FIG. 1. (Color online) Experimental setup and numerical simulations. (a) The schematic shows the relative position of the QD and the cavity on a wavelength axis. For the particular QD-cavity system considered, the QD is red detuned from the cavity, though off-resonant coupling is observed for both red and blue detuned QDs. In experiments, a strong pump laser dresses the QD while a weak probe laser is scanned across the QD. QD emission is incoherently coupled to the cavity. The cavity emission is monitored as a function of probe laser wavelength  $\lambda_p$ . (b) The experimental setup is a confocal cross-polarization setup. The PBS (polarizing beam splitter) is used to perform cross-polarized reflectivity measurements, as in previous work (Ref. 3). The powers are measured in front of the objective lens (OL). The output is dispersed in a single-grating monochromator and measured by a nitrogen-cooled CCD. We employ a linear three hole defect PC cavity (a scanning electron micrograph is shown in the inset). (c) Normalized off-resonant cavity emission obtained by numerical simulation is plotted as a function of  $\lambda_p - \lambda_{QD}$ ,  $\lambda_{QD}$  and  $\lambda_p$  being the QD resonance and probe laser wavelengths, respectively, for different pump powers  $P$  (normalized units), while the probe power is kept at 1. The pump laser is resonant with the QD. (d) For a pump power of  $P = 25$ , the cavity emission is plotted as a function of  $\lambda_p - \lambda_{QD}$  for different pump-QD detunings  $\Delta\lambda_{\text{pump}}$  (nm). In both (c) and (d), spectra are vertically offset for clarity.

decay with a rate  $2\kappa$ . The two terms with  $\gamma_r$  represent a phonon-mediated coupling between the cavity and the QD.<sup>7</sup> The last term with  $\gamma_d$  phenomenologically describes pure dephasing of the QD. We numerically calculate the emission spectrum of the cavity given by the Fourier transform of the two-time correlation function of the cavity field, proportional to  $\langle a^\dagger(\tau)a(0) \rangle$ . Under the quantum regression theorem the autocorrelation function is equal to  $\text{tr}\{a^\dagger M(\tau)\}$  where  $M(\tau)$  obeys the master equation with initial condition  $a\rho(t \rightarrow \infty)$ . The time dependence of the Hamiltonian is such that the master equation can be cast in terms of Liouvillian superoperators as

$$\dot{\rho} = (\mathcal{L}_0 + \mathcal{L}_+ e^{i\delta t} + \mathcal{L}_- e^{-i\delta t})\rho. \quad (3)$$

This equation is solved with Floquet theory, by assuming a solution of the form  $\rho(t) = \sum_{n=-\infty}^{\infty} \rho_n(t) e^{in\delta t}$ . The number

of terms in the expansion necessary to obtain any level of precision is determined by the relative strength of  $J_1$  to  $J_2$ , and in this way the problem can be considered perturbative in the probe strength.

Introducing this trial solution to Eq. (3), taking the Laplace transform, and equating terms proportional to  $e^{in\delta t}$  yields the recurrence relation

$$z\rho_n(z) + \rho(0)\delta_{n0} + in\delta\rho_n(t) = \mathcal{L}_0\rho_n(z) + \mathcal{L}_+\rho_{n-1}(z) + \mathcal{L}_-\rho_{n+1}(z), \quad (4)$$

which can be solved numerically by the method of continued fractions. We seek the resonance fluorescence spectrum of the cavity which is found as the real part of the Fourier transform of the stationary two-time correlation function  $\langle a^\dagger(t + \tau)a(t) \rangle$ . Application of the quantum regression theorem allows this quantity to be calculated as  $\text{tr}\{a^\dagger M(\tau)\}$ , where  $M(\tau)$  solves the master equation with initial condition  $M(0) = a\rho(t \rightarrow \infty)$ . From the recurrence relation and the aforementioned initial condition the method of continued fractions allows us to obtain an expansion of the Laplace transform of  $M(\tau)$  of the form

$M(z) = \sum_{n=-\infty}^{\infty} M_n(z + in\delta)$ , from which the cavity resonance fluorescence spectrum is

$$S(\omega) = \text{Re}(\text{tr}\{a^\dagger M_0(i\omega)\}), \quad (5)$$

where  $\omega$  is the angular frequency of the emitted light, centered at the frequency of the pump laser. In our calculation,  $\rho_0$  is found to first order in  $J_2$  by assuming all  $\rho_n$  for  $|n| > 1$  are 0, reflecting the relatively weak probe strength. In the regime under consideration much less than one photon is ever in the cavity at any time (i.e.,  $\langle a^\dagger a \rangle \ll 1$ ) and the photon basis is truncated to a small subspace of Fock states ( $|0\rangle, |1\rangle, |2\rangle$ ). These approximations are validated by observing no change in the calculation with an expansion of either basis.

For all the simulations we use the numerical integration routines provided in the quantum optics toolbox.<sup>12</sup> The height of the peak at the cavity resonance is calculated as a function of the probe detuning  $\delta$ . The criterion for the appearance of dressed states is that the pump Rabi frequency  $J_1$  should be higher than the QD linewidth  $2\gamma$ . The inclusion of incoherent terms  $\gamma_r$  and  $\gamma_d$  effectively broadens the dot and alters this condition, but below a certain critical value of  $J_1$  the change in the cavity height with probe detuning is a simple Lorentzian with a linewidth on the order of the natural QD linewidth. Above threshold, the dressed states are resolvable and the cavity height spectrum splits into two peaks in the experimental regime we considered. Broadening of the peaks in the experiment beyond the theoretical prediction is caused by spectral diffusion of the QD, which likely arises from the charge fluctuations on etched surfaces of the photonic crystal. The parameters used for the simulations are  $\kappa/2\pi = 17$  GHz,  $\gamma/2\pi = 1$  GHz,  $\gamma_r/2\pi = 0.5$  GHz,  $\gamma_d/2\pi = 3$  GHz,  $\Delta = 8\kappa$ , and  $\bar{n} = 1$ . In these simulations we neglect any coherent coupling between the QD and the cavity (i.e., the coherent dot-cavity coupling strength  $g = 0$ ). Figure 1(c) shows the theoretically calculated cavity output as a function of the probe laser wavelength  $\lambda_p$  for different powers  $P$  of the resonant pump laser. At low pump power, we observe a simple Lorentzian line shape with QD linewidth.<sup>8</sup> However,

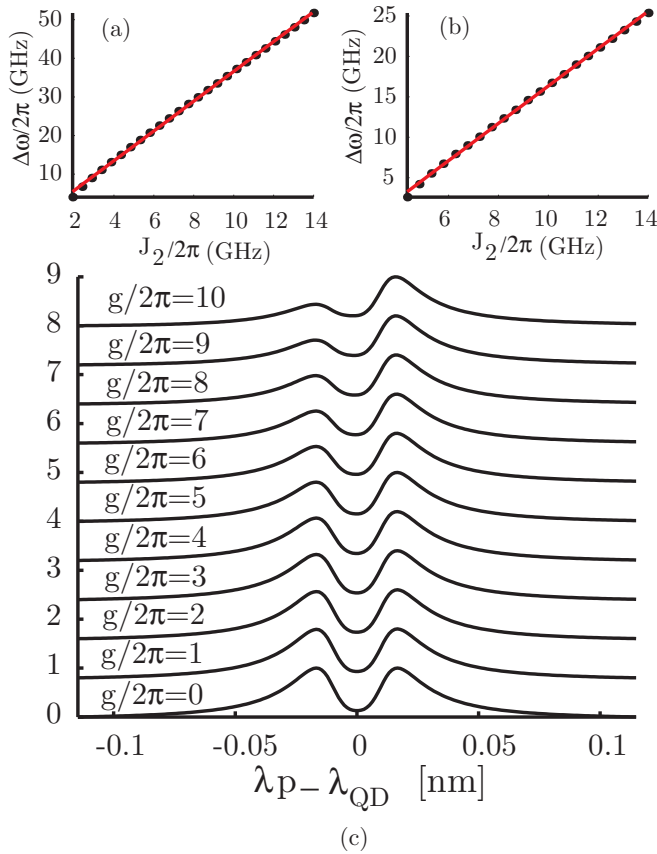


FIG. 2. (Color online) Power dependence of the peaks and dips in the cavity emission spectra and effect of coherent dot-cavity interaction strength  $g$ : (a) The separation between the two peaks [as shown in Fig. 1(c)] as a function of the laser Rabi frequency. The slope of the linear fit is  $\sim 4$ . (b) The separation between the two dips [as shown in Fig. 1(c)] as a function of the laser Rabi frequency. The slope of the linear fit is  $\sim 2$ . (c) Cavity emission as a function of probe laser wavelength, for different dot-cavity coupling  $g$ .

as the pump power is increased, the Lorentzian peak splits into two peaks, the separation between the peaks increasing linearly with pump Rabi frequency. We find that these two peaks are separated by  $\sim 4$  times the Rabi frequency  $J_2$  [Fig. 2(a)]. As the pump power is increased further, a third peak corresponding to the central Mollow peak appears at the QD resonance, leading to the emergence of two dips whose separation also increases linearly with pump Rabi frequency [Fig. 2(b)].

We note that the lack of a prominent central Mollow peak as observed in resonance fluorescence studies of single QDs<sup>13,14</sup> is a result of the saturation of the QD absorption and, hence, of the cavity emission. As such, these cavity emission measurements are more akin to absorption measurements of a strongly driven QD<sup>15,16</sup> rather than the aforementioned resonance fluorescence measurements.<sup>13,14</sup> Figure 1(d) plots the cavity output for different detunings  $\Delta\lambda_{\text{pump}} = \lambda_{\text{pump}} - \lambda_{\text{QD}}$  between the pump and the QD. We observe that the two peaks remain distinct but become asymmetric when the pump is detuned from the QD. This is consistent with the anticrossing of the Rabi sidebands of the dressed QD that occurs as the pump is tuned through the QD resonance.<sup>17</sup> Inclusion of  $g$  makes the two peaks asymmetric. Figure 2(c)

shows the cavity emission for a pump power of 25, with  $g/2\pi$  ranging from 0 to 10. Here the cavity is at a shorter wavelength compared to the QD, and we observe that the peak closer to the cavity is not enhanced. This observation is starkly different from the resonance fluorescence measurement, where the peak close to the cavity is enhanced, as observed in Refs. 17 and 18. This indicates, again, that this way of measuring the coherent interaction between the QD and the laser is akin to an absorption measurement. These theoretical results demonstrate that measurements of cavity emission allow for the observation of phenomena associated with the coherent optical driving of the QD.

### III. EXPERIMENT

To demonstrate the use of such cavity emission to perform coherent optical spectroscopy of an off-resonantly coupled QD, we perform a series of experiments measuring the optical emission spectra of a system consisting of a single self-assembled InAs QD off-resonantly coupled to a linear three hole defect GaAs PC cavity kept at cryogenic temperatures in a helium-flow cryostat ( $\sim 30\text{--}35$  K) [Fig. 1(b)].<sup>3</sup> The 160 nm GaAs membrane used to fabricate the photonic crystal is grown by molecular beam epitaxy on top of a GaAs (100) wafer. A low-density layer of InAs QDs is grown in the center of the membrane (80 nm beneath the surface). The GaAs membrane sits on a 918 nm sacrificial layer of  $\text{Al}_{0.8}\text{Ga}_{0.2}\text{As}$ . Under the sacrificial layer, a 10-period distributed Bragg reflector, consisting of a quarter-wave AlAs/GaAs stack, is used to increase collection into the objective lens. The photonic crystal was fabricated using electron beam lithography, dry plasma etching, and wet etching of the sacrificial layer in diluted hydrofluoric acid, as described previously.<sup>3</sup>

Experiments are performed by driving the QD-cavity system under different optical configurations and measuring optical emission. Optical emission is collected and dispersed by a single-grating monochromator and then measured by a liquid-nitrogen-cooled charge-coupled device (CCD). We first characterize the coupled QD-cavity system by measuring the photoluminescence (PL) spectrum obtained under above-band excitation by an 820 nm Ti:sapphire laser [Fig. 3(a)]. From the Lorentzian fit to the cavity resonance, we find that the cavity linewidth is  $\Delta\lambda_{\text{cav}} = 0.1$  nm, corresponding to a cavity field decay rate of  $\kappa/2\pi = 17$  GHz. We do not observe the anticrossing of the cavity and QD peaks when the QD is tuned across the cavity resonance by changing temperature, indicating that the QD is not strongly coupled to the cavity. The QD resonance is at  $\lambda_{\text{QD}} = 927.5$  nm and the cavity resonance is at  $\lambda_{\text{cav}} = 927.1$  nm at 35 K temperature leading to a dot-cavity detuning  $\Delta\lambda = \lambda_{\text{QD}} - \lambda_{\text{cav}} = 0.4$  nm. Once these system parameters are determined, we confirm the presence of off-resonant coupling effects by scanning a narrow-bandwidth CW field in wavelength across the QD-cavity system and measuring emission spectra, as shown in Fig. 3(b). In these spectra, off-resonant coupling leads to the observation of cavity emission under optical excitation of the QD and vice versa. We note that these emission signatures depend on the polarization of the scanning laser and are maximum when the laser is co-polarized with the PC cavity mode. We can estimate the linewidth of the QD ( $\Delta\lambda_{\text{QD}} = 0.06$  nm) and

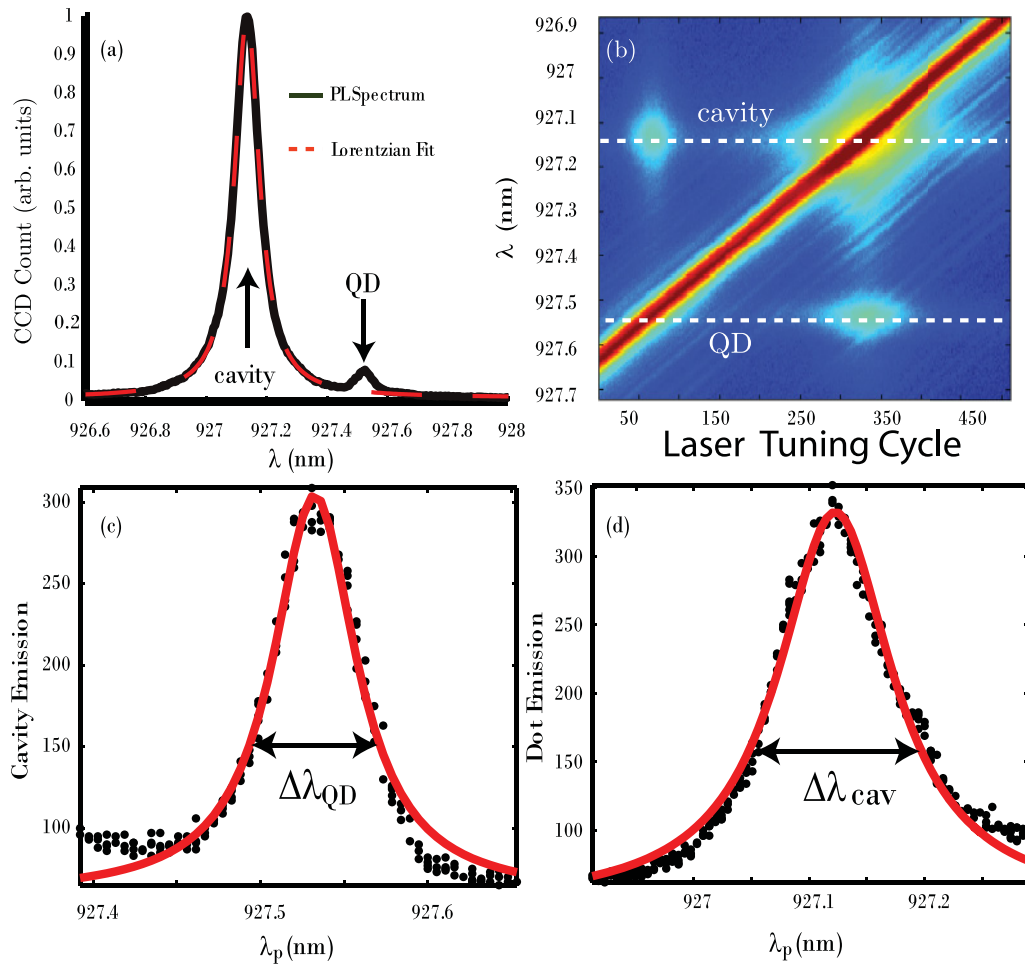


FIG. 3. (Color online) Characterization of the QD-cavity system in photoluminescence (PL) and probing of the off-resonant dot-cavity coupling. (a) PL spectrum of the system. From the Lorentzian fit to the cavity we estimate a cavity linewidth  $\Delta\lambda_{cav} = 0.1$  nm. (b) The laser is scanned across the QD-cavity system. Emission from the cavity is observed when the laser is resonant with the QD. Similarly, emission from the QD is observed when the laser is resonant with the cavity. (c), (d) The QD (cavity) linewidth is measured by monitoring the cavity (QD) emission as a function of the probe wavelength  $\lambda_p$ .

the cavity ( $\Delta\lambda_{cav} = 0.11$  nm) by scanning the excitation laser across one resonance and observing emission at the other [Figs. 3(c) and 3(d)]. These measurements yield a broader cavity linewidth compared to that measured in standard PL measurements due to the heating of the structure caused by the resonant laser.<sup>8</sup> We now use this off-resonant cavity emission to probe the dressing of the QD by a strong resonant laser field.

To observe the QD dressed states, we scan the CW (probe) field across the QD resonance and measure the cavity emission signal [as in Fig. 3(c)] in the presence of a strong CW pump field tuned resonantly to the QD transition. The pump laser, co-polarized with the probe laser, serves to dress the QD, thus qualitatively altering the observed cavity emission spectrum. To optimize the signal to noise ratio of cavity emission measurements, the polarization of the pump and probe fields is rotated 45 degrees with respect to the cavity mode polarization in front of the objective lens to minimize the amount of pump and probe light collected through the polarizing beam splitter (PBS) [Fig. 1(b)]. High amounts of collected excitation light lead to higher noise in cavity emission as measured by the spectrometer CCD even when the cavity and the QD are

detuned. Figure 4(a) shows the cavity emission intensity as a function of the probe laser wavelength  $\lambda_p$ . In the absence of the pump laser ( $P = 0$ ), we observe that the cavity emission spectrum possesses a Lorentzian line shape. However, when a strong pump drives the QD, the Lorentzian splits into two peaks, as observed in the simulations in Fig. 1(c). However, experimentally measured QD linewidths are broadened by spectral diffusion of the QD transition, which is not included in our theoretical model.<sup>19</sup> Hence, we fit a Lorentzian to each peak and study the splitting between two peaks as a function of the pump laser power. Figure 4(b) plots this splitting as a function of the square root of the laser power  $P$  measured in front of the objective lens (OL). We observe that the splitting increases linearly with  $\sqrt{P} \propto E$ , the laser field amplitude. The splitting is given by  $\sim 4$  times the laser Rabi frequency  $\Omega = \vec{\mu}_d \cdot \vec{E}/\hbar$ , where  $\mu_d$  is the QD dipole moment. We note that in the results of Fig. 4(a), the peaks are not symmetric. This is mainly due to the fact that fixing the pump laser exactly to the QD resonance in experiments is made difficult by spectral drifts in both the QD resonance and the pump laser wavelength over time. However, this asymmetry can also

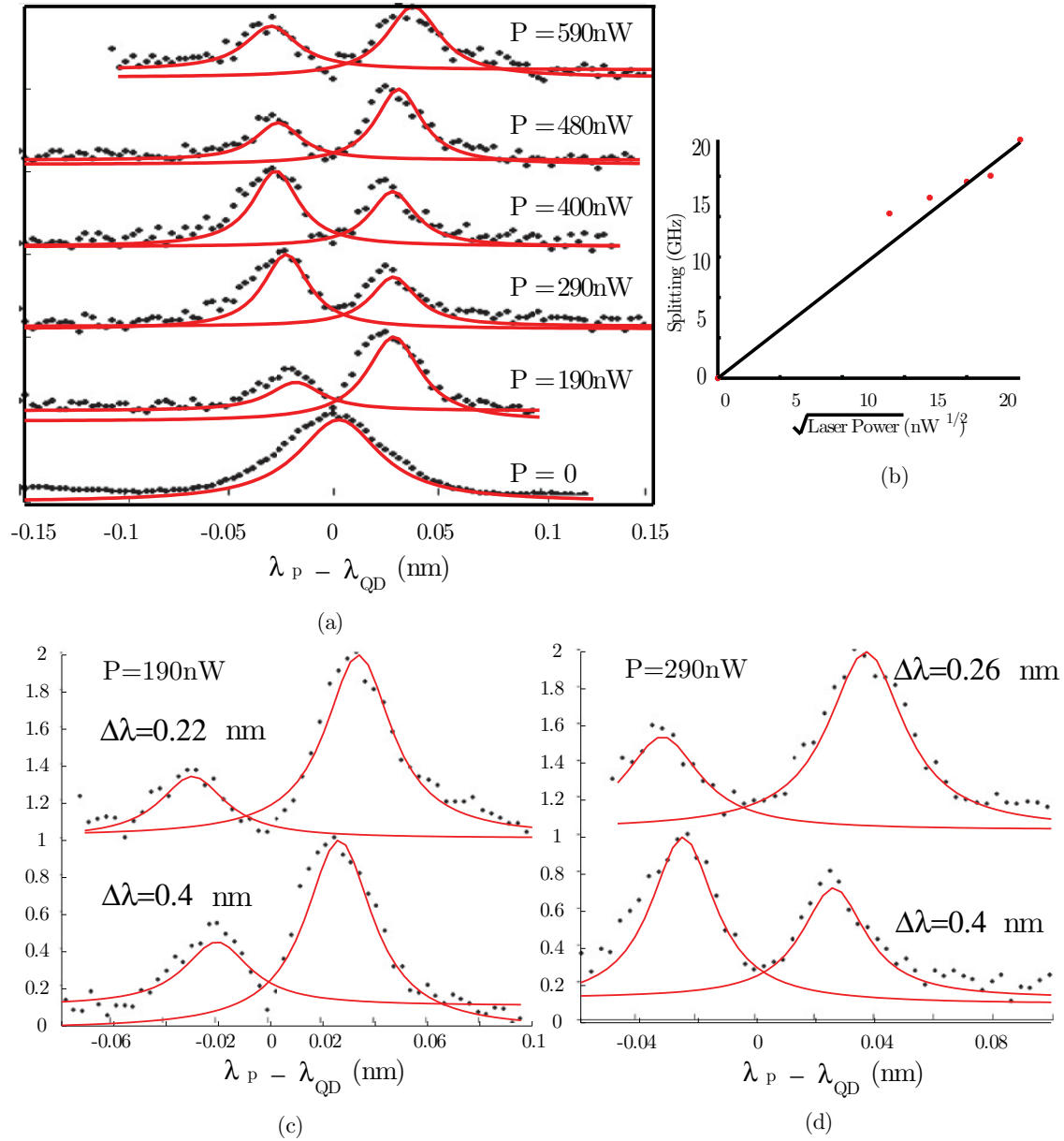


FIG. 4. (Color online) Coherent interaction between the QD and the laser observed through cavity emission. (a) Normalized cavity emission as a function of the probe laser wavelength for different pump powers (measured before the objective lens). We observe that a single QD resonance splits into two peaks. The splitting is linearly proportional to the Rabi frequency of the pump laser. Each peak is fitted with a Lorentzian. (b) Rabi frequency  $\Omega$  of the laser (estimated from the splitting) as a function of the square root of the pump power  $P$ . A linear relation exists between  $\Omega$  and  $\sqrt{P}$ . (c) Normalized cavity emission for a pump power of 190 nW for two different QD-cavity detunings  $\Delta\lambda = 0.22$  and 0.4 nm. (d) Cavity emission for a pump power of 290 nW at two different QD-cavity detunings  $\Delta\lambda = 0.26$  and 0.4 nm. We observe that the splitting increases for smaller detuning (i.e., when the pump laser is closer to the cavity), which suggests that the input laser power is enhanced by the presence of the cavity. For all experiments the probe laser power is kept constant at 20 nW. The QD-cavity detuning is defined as  $\Delta\lambda = \lambda_{QD} - \lambda_{cav}$ . In (a), (c), and (d) the spectra are vertically offset for clarity.

be partially attributed to the coherent interaction  $g$  between the QD and the cavity [Fig. 2(b)]. For a detuned pump, the splitting is modified, and this causes a deviation of the Rabi frequencies from the linear relation as shown in Fig. 4(b). We also note that the high pump power regime of Fig. 1(c), which shows a central peak and two dips in the observed spectra, is difficult to observe in experiments due to the fact that there is still considerable pump leakage through the PBS. At higher powers, this transmitted pump light can saturate CCD pixels

corresponding to wavelengths near the pump wavelength. This saturation can result in charge leakage across CCD pixels leading to a deterioration of the signal to noise ratio of cavity emission measurements. The use of improved spectral filtering techniques would reduce the amount of pump light collected, possibly enabling observation of this high-power regime.

We estimate that the off-resonant cavity ( $\Delta\lambda = 0.4$  nm) enhances the laser electric field inside cavity by a factor of  $\sim 40$ , compared to the bare QD case, assuming a spot size of

3  $\mu\text{m}$  and QD at the field maximum (see the appendices). This agrees with the result shown in Fig. 4(c), where the cavity emission is plotted for two different QD-cavity detunings at the same pump power. The Rabi frequencies of the laser at a QD-cavity detuning of  $\Delta\lambda = 0.4$  nm are measured to be 8.15 and 8.9 GHz at input powers of 190 and 290 nW, respectively. The Rabi frequencies increase to 11.1 and 12.1 GHz when the pump is closer to the cavity resonance ( $\Delta\lambda$  are 0.26 and 0.22 nm, respectively). We theoretically estimate these Rabi frequencies to be 11.6 and 13.8 GHz, which are close to the experimentally measured values.

Finally, we study the effects of the detuning between the pump and the QD resonance on the off-resonant cavity emission. Figure 5 shows the cavity emission as a function of probe laser wavelength  $\lambda_p$  for different pump laser–QD detunings  $\Delta\lambda_{\text{pump}} = \lambda_{\text{pump}} - \lambda_{\text{QD}}$ . The pump laser power is kept fixed at 290 nW. The detuning  $\Delta\lambda_{\text{pump}}$  is changed from  $-0.04$  nm (blue detuned) to  $0.04$  nm (red detuned). We observe that when the pump laser is far detuned from the QD resonance, the cavity emission shows a single peak with  $\lambda_p$ . As the pump is tuned closer to the cavity resonance, two peaks emerge in the spectrum, where the peaks are asymmetric when the pump is not exactly resonant with the QD. The fact that the peaks remain distinct as the pump is tuned through the QD resonance verifies experimental observation of the anticrossing of the Rabi sidebands of the driven QD, consistent with the theory [Fig. 1(d)].

#### IV. CONCLUSION

In conclusion, we demonstrate that signatures of the coherent driving of a QD by a strong pump laser are preserved after phonon-assisted scattering to an off-resonant cavity

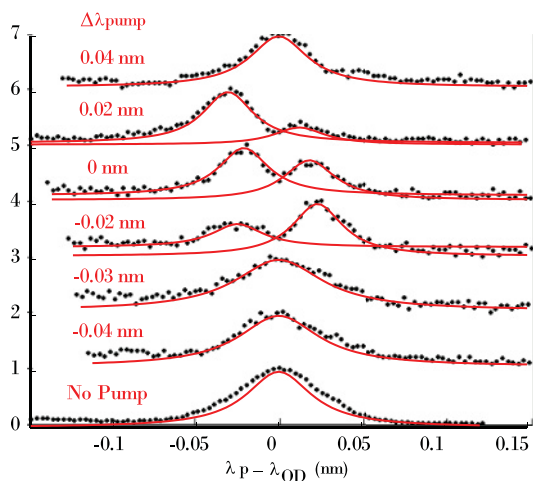


FIG. 5. (Color online) Dependence of the result on pump-QD detuning. Off-resonant cavity emission as a function of the probe laser wavelength for different pump-QD detunings  $\Delta\lambda_{\text{pump}} = \lambda_{\text{pump}} - \lambda_{\text{QD}}$ . We observe that the QD linewidth broadens when the pump is present and detuned from the QD resonance. As the pump is tuned through the QD resonance, we observe the emergence of two peaks in the cavity emission spectrum. This two-peak spectrum is consistent with the observation of the anticrossing of Rabi sidebands. The pump and probe power are kept at 290 nW and 20 nW, respectively. The spectra are offset for clarity.

despite the fact that this scattering process is incoherent. In addition to revealing new aspects of the off-resonant QD-cavity interaction, this result is also potentially useful for enabling simpler coherent optical spectroscopy of a QD, as the readout signal is offset in frequency and can be spectrally filtered using well-established techniques. Moreover, this approach may relax the requirement of working exclusively with strongly coupled QD-cavity systems in quantum networks.

#### ACKNOWLEDGMENTS

The authors acknowledge financial support provided by the Army Research Office, Office of Naval Research, and National Science Foundation. A.M. was supported by a Stanford Graduate Fellowship (Texas Instruments Fellowship). E.K. was supported by an Intelligence Community (IC) Postdoctoral Research Fellowship.

#### APPENDIX A: ESTIMATION OF ELECTRIC FIELD ENHANCEMENT

We consider a Gaussian laser beam with power  $P$  and frequency  $\omega$  incident on a photonic crystal cavity. The power is measured in front of the objective lens and the coupling efficiency of the laser to the cavity is  $\eta$ . If the cavity quality factor is  $Q = \omega_0/\Delta\omega$ , with cavity resonance frequency  $\omega_0$  and linewidth  $\Delta\omega$ , the energy inside the cavity (for a laser resonant to the cavity) is  $W = P\eta/\Delta\omega$ . For an off-resonant cavity, where the laser is detuned from the cavity by  $\Delta$ , the previous expression for energy is multiplied by a Lorentzian:

$$f = \frac{1}{1 + (2\Delta/\Delta\omega)^2}, \quad (\text{A1})$$

where  $\Delta = \omega - \omega_0$  with  $\omega_0$  being the resonance frequency of the cavity. The energy in the cavity can also be expressed as  $\epsilon|E_{\text{max}}|^2V_m$ , where  $\epsilon$  is the permittivity of the medium, and  $E_{\text{max}}$  is the electric field at the point of maximum electric energy density, and  $V_m$  is the cavity mode volume. Equating the two expressions of energy, we can write

$$\frac{P\eta}{\Delta\omega} \frac{1}{1 + (2\Delta/\Delta\omega)^2} = \epsilon|E_{\text{max}}|^2V_m. \quad (\text{A2})$$

Using

$$\Delta\omega = \frac{\omega_0}{Q} = \frac{2\pi c}{Q\lambda_0}, \quad (\text{A3})$$

where  $c$  is the velocity of light and  $\lambda_0$  is the resonance wavelength of the cavity, we can find  $E_{\text{max}}$ :

$$|E_{\text{max}}| = \sqrt{\frac{\eta P Q \lambda_0}{2\pi c \epsilon V_m} \frac{1}{1 + (2\Delta/\Delta\omega)^2}}. \quad (\text{A4})$$

If the quantum dot is not located at the point of the maximum electric field energy density, the electric field at its location will be smaller than  $E_{\text{max}}$  [and the spatial variation of the  $E$  field is determined by the mode pattern  $\psi(x, y)$ ]. Therefore, the electric field at the location of the QD would be

$$|E_{\text{cav}}| = |E_{\text{max}}|\psi(x, y). \quad (\text{A5})$$

On the other hand, when there is no cavity present, the intensity  $I$  of the light (assuming a Gaussian beam) incident on the GaAs is given by

$$I = \frac{P}{2\pi\sigma_0^2}, \quad (\text{A6})$$

where  $\sigma_0$  is the Gaussian beam radius of the laser. Also the intensity of the laser is given by

$$I = \frac{1}{2}c\epsilon|E|^2. \quad (\text{A7})$$

Equating these two, the electric field is found to be

$$|E| = \sqrt{\frac{P}{c\epsilon\pi\sigma_0^2}}. \quad (\text{A8})$$

Assuming normal incidence on the air-GaAs interface,

$$|E_{\text{GaAs}}| = \frac{2}{1+n}|E|, \quad (\text{A9})$$

where  $n$  is the refractive index of GaAs. We note that the effect of the reflection in the interface is embedded in  $\eta$  for the analysis done for the cavity. From the above discussion, the electric field sensed by the QD in the absence of the cavity has the form

$$|E_{\text{no cav}}| = \frac{2}{1+n}\sqrt{\frac{P}{c\epsilon\pi\sigma_0^2}}. \quad (\text{A10})$$

Comparing the cavity and no-cavity case, we can find that the electric field enhancement is given by

$$\frac{E_{\text{cav}}}{E_{\text{no cav}}} = \frac{1+n}{2}\sqrt{\frac{\eta Q\lambda_0\sigma_0^2}{2V_m} \frac{1}{1+(2\Delta/\Delta\omega)^2}}\psi(x,y). \quad (\text{A11})$$

When the laser is resonant with the cavity, the maximum field enhancement for a linear three hole defect ( $L_3$ ) cavity is  $\sim 350$ , assuming  $\eta = 1\%$ ,  $Q = 10\,000$ ,  $\lambda_0 = 927$  nm,  $\sigma_0 = 3$   $\mu\text{m}$ ,  $V_m = 0.8(\lambda_0/n)^3$ , and the QD at the field maximum, i.e.,  $\psi = 1$ . For a detuning of 4 linewidths (as is true for our experiment), the maximum enhancement is  $\sim 40$ . We note that this maximum enhancement can be increased by using a cavity with a higher quality factor or lower mode volume. Another way to increase the enhancement is by increasing the coupling efficiency  $\eta$  by using a waveguide or a fiber coupled to the cavity.

## APPENDIX B: ESTIMATION OF THE QD DIPOLE MOMENT

The data of Figs. 3(a) and 3(b) allow for order of magnitude estimation of system parameters such as QD dipole moment and effective QD electric field. Assuming a coupling efficiency of the Gaussian laser beam to the PC cavity mode  $\eta$ , we can estimate the maximum laser field amplitude  $E$  at the position of the QD using Eq. (A4). From the linear fit in Fig. 3(b), we estimate the dipole moment  $\mu_d$  of the QD to be on the order of 22 D, with  $\eta = 1\%$  as obtained previously with the same grating coupled cavity design.<sup>20</sup> For this dipole moment, the maximum QD-cavity interaction strength  $g/2\pi$  should be  $\sim 29$  GHz, assuming the QD is located at the electric field maximum, thereby leading to the strong coupling. As mentioned previously, we did not observe the anticrossing of the QD and cavity peaks in PL and thus believe that the actual value of  $g$  is smaller than this calculated value most likely because the QD is not located at the cavity electric field maximum.

\*arkam@stanford.edu

<sup>1</sup>D. Press, T. D. Ladd, B. Zhang, and Y. Yamamoto, *Nature (London)* **456**, 218 (2008).

<sup>2</sup>E. D. Kim, K. Truex, X. Xu, B. Sun, D. G. Steel, A. S. Bracker, D. Gammon, and L. J. Sham, *Phys. Rev. Lett.* **104**, 167401 (2010).

<sup>3</sup>D. Englund, A. Faraon, I. Fushman, N. Stoltz, P. Petroff, and J. Vučković, *Nature (London)* **450**, 857 (2007).

<sup>4</sup>D. Englund, A. Majumdar, A. Faraon, M. Toishi, N. Stoltz, P. Petroff, and J. Vučković, *Phys. Rev. Lett.* **104**, 073904 (2010).

<sup>5</sup>S. Ates, S. M. Ulrich, A. Ulhaq, S. Reitzenstein, A. Löffler, S. Höfling, A. Forchel, and P. Michler, *Nature Photonics* **3**, 724 (2009).

<sup>6</sup>U. Hohenester, *Phys. Rev. B* **81**, 155303 (2010).

<sup>7</sup>A. Majumdar, E. Kim, Y. Gong, M. Bajcsy, and J. Vučković, *Phys. Rev. B* **84**, 085309 (2011).

<sup>8</sup>A. Majumdar, A. Faraon, E. D. Kim, D. Englund, H. Kim, P. Petroff, and J. Vučković, *Phys. Rev. B* **82**, 045306 (2010).

<sup>9</sup>A. Ulhaq, S. Ates, S. Weiler, S. M. Ulrich, S. Reitzenstein, A. Löffler, S. Höfling, L. Worschech, A. Forchel, and P. Michler, *Phys. Rev. B* **82**, 045307 (2010).

<sup>10</sup>H. F. Z. Ficek, *Phys. Rev. A* **53**, 4275 (1995).

<sup>11</sup>C. W. Gardiner and P. Zoller, *Quantum Noise* (Springer-Verlag, 2005).

<sup>12</sup>S. M. Tan, *J. Opt. B* **1**, 424 (1999).

<sup>13</sup>E. B. Flagg, A. Muller, J. W. Robertson, S. Founta, D. G. Deppe, M. Xiao, W. Ma, G. J. Salamo, and C. K. Shih, *Nature Phys.* **5**, 203 (2009).

<sup>14</sup>A. N. Vamivakas, Y. Xhao, C. Lu, and M. Atature, *Nature Phys.* **5**, 198 (2009).

<sup>15</sup>X. Xu, B. Sun, P. R. Berman, D. G. Steel, A. S. Bracker, D. Gammon, and L. J. Sham, *Science* **317**, 929 (2007).

<sup>16</sup>G. Jundt, L. Robledo, A. Högele, S. Fält, and A. Imamoglu, *Phys. Rev. Lett.* **100**, 177401 (2008).

<sup>17</sup>X. Xu, B. Sun, E. D. Kim, K. Smirl, P. R. Berman, D. G. Steel, A. S. Bracker, D. Gammon, and L. J. Sham, *Phys. Rev. Lett.* **101**, 227401 (2008).

<sup>18</sup>C. Roy and S. Hughes, *Phys. Rev. Lett.* **106**, 247403 (2011).

<sup>19</sup>H. Kamada and T. Kutsuwa, *Phys. Rev. B* **78**, 155324 (2008).

<sup>20</sup>M. Toishi, D. Englund, A. Faraon, and J. Vučković, *Opt. Express* **17**, 14618 (2009).